Acoustical Noise Analysis and Prediction by means of Multiple Seasonality Time Series Model

Claudio Guarnaccia, Joseph Quartieri, Eliane R. Rodrigues, Carmine Tepedino

***Abstract*—**Physical polluting agents are a relevant problem in urban areas. The need for monitoring and prediction of their time evolution is very useful to assess the impact to human health and activities. Considering their effects on health, the most hazardous agents to be considered are air pollution, acoustical noise and electromagnetic fields. Regarding acoustical noise, the complexity of predicting its slope is strongly correlated to its intrinsic randomness, related to the great variability of the sources. Sometimes, in some special areas, the predominant sources are stationary or have a periodic behaviour. In these cases, a time series analysis approach can be adopted, considering that a general trend and a local periodicity can be highlighted and used to build a predictive model. In particular, in this paper, the model is built composing three parts: the trend, that is the long term behaviour, the seasonality, that is the periodic component, and the irregularity, that includes the random variations. Applying such a model to a traffic noise levels dataset, obtained from a site in the city of Messina, Italy, a multiple seasonality is evidenced, resulting in two seasonal coefficients introduction (low frequency and high frequency). The validation of the presented model will be performed on a 44 days dataset, not used in the calibration. Results will be encouraging and will show a very good prediction performances of the model, especially in terms of difference between observed and simulated values (error). The error distributions will be analyzed and discussed by means of statistical indexes, plots and tests.

***Keywords*—**Time Series, Acoustics, Noise Control, Predictive Model.

I. Introduction

POPULATION of large urban areas have their health often affected by several adverse effects caused by various forms of pollution [1-3]. The constant monitoring of these pollutants is generally expensive and not always easy to be implemented [4]. In addition, mitigation actions on the sources are usually consequential to periods in which the level of pollution has been particularly high and therefore has already affected the citizens' health. These considerations point out the need to implement predictive models that can provide a reliable assessment of pollution levels (see for instance [5-28]). These models can induce possible mitigation measures, acting also on the sources, before the pollution begins to affect the population.

In this work, the focus is on the prediction of acoustical noise level in urban areas. That is mainly generated by anthropogenic activities, in particular vehicular traffic and other transport infrastructures.

Most of the existing forecasting models used to estimate pollution levels are based on the study of correlations or causal effects derived from the sources. However, because of the nature of the physical phenomenon in the case of acoustical noise, it is very difficult to predict the effects in a limited area by studying only the sources. That can be heavily influenced either by the architecture of the area where measurements are taken or by other environmental interferences highly variable over time.

The forecasting model considered here is based on time series analysis (TSA) [29-32], applied to sound level measurements. The model can predict the evolution of noise levels for a certain time interval, in a specific area of interest, i.e. the area in which the data used for the estimation of the parameters (tuning) of the forecasting function have been collected. This function is known in its general form, but it can be adapted to the specific data to get more accurate forecasted values. In particular, the simplest functional forms of the model can be used with success when there are few measurements available to estimate the parameters. Moreover, if a large tuning data set is available, it is possible to implement more complex models to reduce the forecast error.

In particular, in this study a set of noise measurements recorded at night in the city of Messina, in South Italy, is used. These data consist of equivalent sound pressure levels ($L_{A,eq}$), averaged on the eight night hours (from 10pm to 6am), and they are defined as follows:

$$L_{Aeq,Te} = 10 \log \left[\frac{1}{\sum t_i} \sum_{i=1}^{n} \left(10^{\frac{L_{Aeq,i}}{10}} t_i \right) \right], \qquad (1)$$

where T_e is the exposition time (from 10pm to 6am), t_i is the single period of the series, i.e. the single day, $L_{A,eq,i}$ is the equivalent level measured in the *i*-th period. The "A" index means that the A-weighting curve has been applied to the data,

C Guarnaccia, J. Quartieri and C. Tepedino, are with the Department of Industrial Engineering, University of Salerno, Via Giovanni Paolo II, I-84084 Fisciano (SA) – ITALY (corresponding: cguarnaccia@unisa.it , quartieri@unisa.it , ctepedino@unisa.it).

E. R. Rodrigues is with the Instituto de Matemáticas, Universidad Nacional Autonóma de México, Mexico City – MEXICO (eliane@math.unam.mx).

ERR was partially supported by the project PAPIIT-IN102713 of the Dirección General de Apoyo al Personal Académico of the Universidad Nacional Autónoma de México, Mexico.

as required by European regulations [33].

The first step consists in constructing a simple but useful model working on the first 321 measurements available. Then, with this model, a 26 missing measurements are filled with forecasted values. That is made in order to have a time series without missing values. This series of 500 data may be used to produce a more sophisticated model. Finally, in order to validate the model, a comparison between actual and forecasted data is performed on the last 44 available measurements. Let us call attention to the fact that the measurements used in the validation have not been used to estimate the parameters. A detailed description on this kind of approach and on the sensibility of the model to the tuning data set, is reported in [34].

II. Methods

The procedure adopted to build the model is based on the general TSA approach. This procedure is used in several research areas such as Economics, Physics, Engineering, Mathematics, among others (see for instance [35-37]).

TSA models reproduce the slope, as a function of time, of a given data series and may be used to predict its values on a certain future time interval. The width of the prediction interval depends on the reliability of the model and on the variability of the series.

The basic assumption of these models is that a time series may be decomposed into three parts: a trend and a seasonality (that are predictable) and an irregular component (not foreseeable) which generates the prediction error. Therefore, for A_t, $t \geq 0$ the series studied, we may write

$$A_t = F_t + e_t \ , \tag{2}$$

where F_t represents the forecasted value at a certain time t, and e_t is the irregular random component.

The ways these parts are composed, for instance by multiplying or adding the components, represent the different types of models. In this work, the multiplicative approach has been pursued, according to the following formula:

$$F_t = T_t \, \bar{S}_i \ , \tag{3}$$

where F_t represents the point forecast, T_t the trend (with t varying over the total number of periods) and $\bar{S}_i$ the seasonal effect (with i varying from 1 to k) at a given time t, averaged on the i-th periods. In particular, for a given t, if $t<k$, the value i is the remainder of the ratio between $t+k$ and k; if $t=k$, then $i=k$; if $t>k$, the value i is the remainder of the ratio between t and k.

The trend component can be evaluated by means of regression techniques, for instance, linear regression on the actual data, or after having removed the seasonality by moving average method. In this work, a linear regression on actual data has been used to calculate the trend. The width of the interval on which the centred moving average is evaluated, depends on the periodicity of the data, also known as lag. This lag is strongly related to the phenomenon under study and its features. In some cases, a multiple periodicity can be highlighted.

In the following sections, it is shown how a TSA model performance improves when a multiple lag is detected and implemented to calculate the forecasted values.

The seasonality is evaluated as the mean, calculated on all the homologous periods, of the ratio between the actual value and the centred moving average in a given time t.

If more than one periodicity is detected, the forecast is affected by another component of seasonality, that is :

$$F_t = T_t \, \bar{S}_{1,i} \, \bar{S}_{2,j} \ , \tag{4}$$

where $\bar{S}_{1,i}$ and $\bar{S}_{2,j}$ are two different seasonal coefficients.

In order to remove the effects of short period seasonality from the data, a centred moving average with width k_1 (first lag detected) can be used. Then, it is possible to evaluate the recurring effect on the single day by the ratio between the actual data at time t and the centred moving average at the same t. Finally, evaluating the mean of these effects $S_{1,t}$ on $m_{1,i}$ homologous periods, the seasonal coefficient $\bar{S}_{1,i}$ is obtained, i.e., for

$$S_{1,t} = \frac{A_t}{M_{(k_1)t}} \ , \tag{5}$$

we have

$$\bar{S}_{1,i} = \frac{\sum_{l=0}^{m_{1,i}-1} S_{1,i+lk_1}}{m_{1,i}} , \tag{6}$$

where $M_{(k_1)t}$ is the centred moving average with width k_1 , at the period t.

At this point, it is possible to clean up the values of the first moving average from the effect of the second seasonality with lag k_2. That is done using a second centred moving average process, with width k_2 (second lag detected). As in the previous step, the effect of the second seasonality for each period ($S_{2,t}$) can be calculated, and a second seasonal coefficient can be evaluated with a mean on $m_{2,j}$ homologous periods:

$$S_{2,t} = \frac{M_{(k_1)t}}{M_{(k_2)t}} \ , \tag{7}$$

$$\bar{S}_{2,j} = \frac{\sum_{l=0}^{m_{2,j}-1} S_{2,j+lk_2}}{m_{2,j}} , \tag{8}$$

where $M_{(k_2)t}$ is the centred moving average with width k_2 , at the period t.

Having assumed the presence of an irregular component, indicated by e_t , its evaluation is given by the difference between actual data and point forecast, i.e. :

$$e_t = A_t - F_t \ . \quad (9)$$

The error is caused by a non-deterministic component of the physical phenomenon under study which the model might fails to predict. This procedure is possible when the actual data are available. Thus it may be performed in the calibration phase. Once the "error" distribution is obtained, its mean (m_e) can be used in the final forecast of the model and the standard deviation can be related to the width of a prediction interval ([32], [34]). Thus the point forecast can be evaluated improving formula (4) as follows:

$$F_t = T_t \bar{S}_{1,i} \bar{S}_{2,j} + m_e \ . \quad (10)$$

A validation process may be performed, comparing actual data with model forecasted values, in a data range not used in the calibration phase.

To evaluate the effectiveness of the model, it is useful to implement a statistical analysis of the errors. This test is performed both in the calibration phase described above and in the validation process. A relevant goal, in order to optimise the model, is to minimise both the absolute value of the mean and the standard deviation of the error distribution.

A. Detection of the presence of a lag

In order to detect the presence of a periodicity in the series, the Ljung-Box (LB) or the Box-Pierce (BP) test can be adopted ([38], [39]). These tests verify if the data have an autocorrelation and they may exclude the presence of fully random data fluctuations. Both tests adopt the autocorrelation coefficient that may be evaluated according to the following formula:

$$r(k) = \frac{\sum_{t=1}^{n-k}(x_t-\bar{x})(x_{t+k}-\bar{x})}{\sum_{t=1}^{n}(x_t-\bar{x})^2} \ , \quad (11)$$

where x_t is the data in each period t, $\bar{x}$ is the mean of all the data, n is the total number of periods, k is the lag hypothesis under test. Using this coefficient, the LB test can be performed according to the following formula:

$$\chi^2_{LB}(h) = n(n+2)\sum_{k=1}^{h}\frac{r^2(k)}{n-k} \ , \quad (12)$$

where h is a chosen integer related to the number of autocorrelation coefficients under test, and it varies according to the assumed lag.

If the null hypothesis is true (absence of autocorrelation), the LB statistics is distributed according to a random variable χ^2, with h degree of freedom.

The BP test is based on the following formula:

$$\chi^2_{BP}(h) = n\sum_{k=1}^{h} r^2(k) \ , \quad (13)$$

where, again, n is the total number of periods, k is the assumed lag and h is a chosen integer, related to the number of autocorrelation coefficients under test. The two tests differ only in the different weighting systems adopted, but asymptotically converge to the same distribution.

B. Selection of the lag coefficient

Once the presence of a periodicity is detected, the choice of the lag may be performed according to the maximum data autocorrelation coefficient.

A very useful tool to detect the periodicity and to evaluate the autocorrelation as a function of the lag, is the autocorrelation plot, also called correlogram. This plot reports the k value on the horizontal axis and the correspondent autocorrelation coefficient on the vertical axis. In this work, since the correlogram has been plotted in the "R" software framework, the autocorrelation coefficients are evaluated according to formula (11).

Let us remind that formula (11) adopts an unique mean calculated on the whole range of data. It may be useful, however, when the time series does not have a constant mean, to adopt the following formula:

$$\rho(k) = \frac{\sum_{t=1}^{n-k}(x_t-\bar{x}_{s1})(x_{t+k}-\bar{x}_{s2})}{\sqrt{\sum_{t=1}^{n-k}(x_t-\bar{x}_{s1})^2}\sqrt{\sum_{t=1}^{n-k}(x_{t+k}-\bar{x}_{s2})^2}} \ , \quad (14)$$

where x_t is the measurement value at time t, n is the number of periods, k is the lag and:

$$\bar{x}_{s1} = \frac{\sum_1^{n-k} x_t}{n-k} \ ; \ \bar{x}_{s2} = \frac{\sum_1^{n-k} x_{t+k}}{n-k} \ . \quad (15)$$

These two means are calculated excluding respectively the first and the last k periods.

In addition, when the lag is particularly high, another possible approach is to evaluate the correlation coefficient between a subset of data and the same data shifted by k periods:

$$r_{xy} = \frac{\sum_{i=1}^{n}(x_i-\bar{x})(y_i-\bar{y})}{(\sum_{i=1}^{n}(x_i-\bar{x})^2)^{\frac{1}{2}}(\sum_{i=1}^{n}(y_i-\bar{y})^2)^{\frac{1}{2}}} \ , \quad (16)$$

where y_i is equal to $x_i + k$.

C. Error metrics

A measurement of model performance can be obtained by "mean percentage error" (MPE) and "coefficient of variation of the error" (CVE). The first quantitative metric gives a measurement of the error distortion, i.e. MPE is able to describe if the model overestimates or underestimates actual data. CVE considers the variation from the reality in absolute value. In other words, it provides the error dispersion. Those metrics are evaluated according to the following formulas:

$$MPE = \frac{\sum_{t=1}^{n}\left(\frac{A_t-F_t}{A_t}\right)100}{n} \quad (17)$$

and

$$CVE = \frac{\sqrt{\frac{\sum_{t=1}^{n}(e_t)^2}{n-1}}}{\bar{A}} \ , \quad (18)$$

where $\overline{A}$ is the mean value of the actual data in the considered time range.

D. Error distribution analysis tools

It is necessary to verify that the mean of the errors (residuals) is not different from zero, in statistical sense. In this paper the authors use the *t*-test:

$$t = \frac{\bar{e}}{s/\sqrt{n}} \quad , \tag{19}$$

where $\bar{e}$ is the mean of the error, *s* is the standard deviation and *n* is the amount of data.

The null hypothesis H_0 is "mean equal to zero". Thus in the numerator of equation (19) there is only the empirical mean (since usually the empirical mean minus the hypothesized one is adopted). In this type of test it is possible to have two type of errors. The first is to reject H_0 when it is true (it can happen with probability α, i.e. the significance level). The second one is to accept H_0 when it is false (this can happen with probability β, and $1 - \beta$ is the power of the test).

It is important to check if the random errors obtained by the model application can be drawn from a normal distribution. To assess the normality of the distribution of errors, the authors proposed both qualitative techniques based on the analysis of graphs such as histogram, QQ normality plot and quantitative indices, namely skewness and kurtosis. In particular, the normal density plot [40] is a graphical technique for assessing whether or not a data set is approximately normally distributed. The data are plotted against a theoretical normal distribution in such a way that the points should form an approximate straight line. Deviations from this straight line indicate deviations from normality.

In addition, the authors adopted the statistical tests of normality from Shapiro-Wilk [41] and Jarque-Bera [42].

The Shapiro-Wilk test (SW) is able to check the normality of a set of data, leading to good results even with a small number of observations. The formula used is:

$$SW = \frac{(a'x)^2}{\sum_{i=1}^{n}(x_i-\bar{x})^2} = \frac{\left(\sum_{i=1}^{n} a_i x_i\right)^2}{\sum_{i=1}^{n}(x_i-\bar{x})^2} \quad , \tag{20}$$

with:

$$a' = (a_1, \ldots, a_n) = \frac{m'V^{-1}}{(m'V^{-1}V^{-1}m)^{1/2}} \quad , \tag{21}$$

where $m' = (m_1, m_2, \ldots, m_n)$ denotes the vector of expected values of standard normal order statistics, and $V = (v_{ij})$ is the corresponding $n \times n$ variance-covariance matrix and $x' = (x_1, x_2, \ldots, x_n)$ denotes a vector of ordered random observations.

The Jarque-Bera test (JB) is often used to verify the hypothesis of normality in the econometric area. It is based on the measurements of the asymmetry and kurtosis of a distribution. The null hypothesis of the test includes two conditions: the skewness and the excess kurtosis should be zero (which means that the kurtosis is 3). If this hypothesis is verified, the data can be considered as derived from a normal distribution, and the JB statistic tends to a chi-squared distribution with two degrees of freedom. The JB test is in general less robust in the application to small samples, leading to often wrongly reject the null hypothesis. The test is based on the following expression:

$$JB = \frac{n}{6}\left(\frac{m_3}{m_2^{\frac{3}{2}}}\right)^2 + \frac{n}{24}\left(\left(\frac{m_4}{m_2^2}\right) - 3\right)^2 \quad , \tag{22}$$

where $m_k = \frac{1}{n}\sum_{i=1}^{n}(x_i - \bar{x})^k$, with $k = 2, 3, 4$.

III. Data Analysis and Results

The basic data set used in this work is related to the Messina's long term field measurements used in [34] and in [43]. The local government of Messina, a city in the South of Italy of about 240000 inhabitants, adopted a continuous monitoring of noise in certain critical areas, particularly in proximity of the commercial dock, where a very high traffic flow and several industrial settlements occur. These data have been made available on a web platform [44] .

In [34] the measurements taken during day time in "Viale Boccetta" street, were used. In this work, the authors adopt the night measurements taken in the same site and, partially, in the same months. In particular, four data sets have been chosen. The first one correspond to the 11th of May 2007 to the 26th of March 2008 (321 days). The second one correspond to the 27th of March 2008 to the 21st of April 2008 (26 days and these data are missing in the data set). The third data set correspond to the 22nd of April 2008 to the 21st of September 2008 (153 days). Finally, the fourth data set, used in the validation phase, correspond to the 22nd of September to the 4th of November 2008 (44 days).

The night level is the equivalent level, with A weighting [33], evaluated in the time range T , that goes from 10pm to 6am (8 hours), defined as follows:

$$L_{Aeq,T} = 10\log\left[\frac{1}{T}\int_0^T \frac{p_A^2(t)}{p_0^2}dt\right] \quad . \tag{23}$$

The first aim of the analysis is to use a forecasting model, tuned on the first series of 321 measurements, to calculate the 26 missing data of the second data set defined above. Then, once the "data hole" has been filled, the same model is tuned on a data set of size 500, composed by the first 321 measurements, plus the 26 reconstructed ones, plus the next 153 measurements. In this way, the last 44 data (from the 501st observed measurement to the 544th) have been left for the validation of the model. The choice of this data set allows the implementation of a multiplicative model with a double seasonal component, which will exploit, in addition to the weekly seasonality ($k_1 = 7$), a second "long term" periodicity ($k_2 = 125$).

The summary statistics of the entire data set are given in Tab. 1.

Table 1: Summary of statistic main parameters of the first 321 days of the data set.

Mean [dBA]	Std.dev [dBA]	Median [dBA]	Min [dBA]	Max [dBA]
68.77	1.19	69.0	66.0	72.0

A. *Seasonality detection and data set filling*

In order to evaluate the presence and the value of the periodicity, the first step was the application of Ljung-Box (LB) and Box-Pierce (BP) tests, defined in (12) and (13). These tests highlight the presence of autocorrelation in the data. The tests have been implemented in the "R" software framework and the results are given in Table 2.

Table 2: Ljung-Box and Box-Pierce tests performed on the first 321 measurements of the dataset.

Type of test	χ^2	h	p-value
Ljung-Box	584.749	10	< 2.2e-16
Box-Pierce	1514.589	50	< 2.2e-16

The small p-value in both tests, i.e. the very small probability to observe the sample if the null hypothesis is true indicates that the hypothesis of absence of autocorrelation in the data must be rejected.

In a first approach using the autocorrelation plot approach, implemented in "R" software the periodicity has been investigated in the first 321 days. The correlogram is reported in Fig.1.

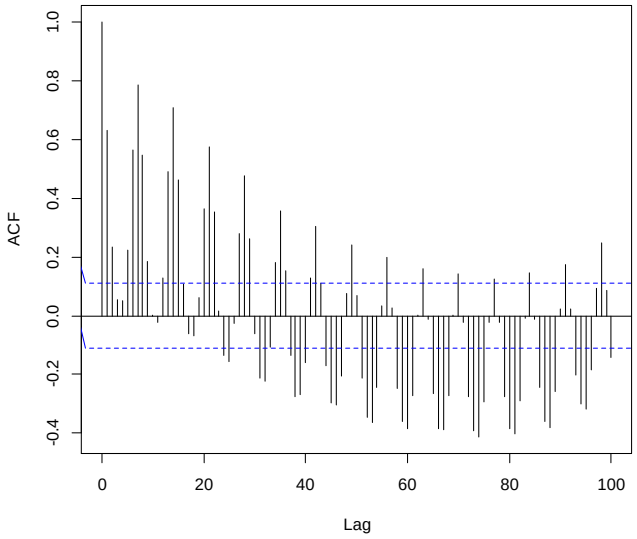

Fig. 1: Correlogram plot for the first 321 days. The value of autocorrelation is plotted as a function of the lag.

The highest autocorrelation value is obtained for a lag of 7 and its value, calculated by means of formula (11), is 0.79 . Thus, it is evident that there is a weekly periodicity in the noise data. This result is reasonable, because the data are strongly related to traffic flows, typically increasing during the working days and decreasing during the weekend.

At this point, a first toy model (single seasonality model, SSM) using the procedure described in section 2 (see also [34]), is implemented considering this lag, i.e. centred moving average for the trend and seasonal coefficient according to a periodicity 7. This model allow the hole in the data set, from day 322 to 348, to be filled, making available a data set of 500 measurements. In Fig. 2 is possible to notice how the data hole has been filled and how the model roughly approximate the actual observed time series.

On this larger dataset (500 days), a second seasonality, with a frequency smaller than the previous one, is hidden and can be highlighted. The autocorrelation of the centred moving average values (with lag 7) has been studied by means of correlogram plot (Fig. 3).

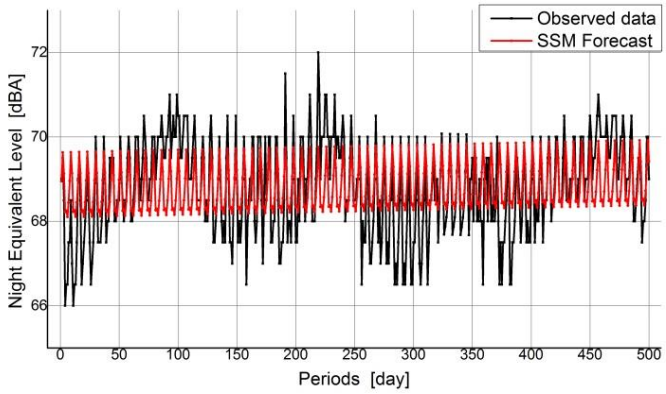

Fig. 2: Comparison between the forecasts, obtained by the single seasonality model (SSM), and the 500 calibration data.

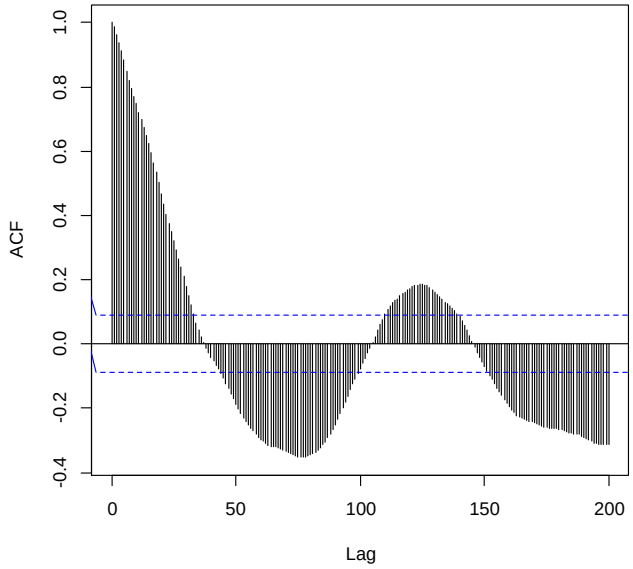

Fig. 3: Correlogram plot for the centred moving average data. The value of autocorrelation coefficient is plotted as a function of the lag.

The correlogram highlights a statistically significant positive autocorrelation for a lag of 125. This autocorrelation has been evaluated according to formula (14), giving a result of 0.20. In the "R" framework, according to formula (11), the results is 0.19. Formula (16) has also been implemented, since it has the advantage of using differences from the mean of the data in a subset whose width is the considered range. In this case, a correlation between the first 50 days and the ones between the 125th and the 175th, has been calculated. The resulting value is 0.55.

In Fig. 4 the auto dispersion plot is reported, considering a lag of 125. The cluster of data along the bisector seems to confirm the presence of autocorrelation in the data.

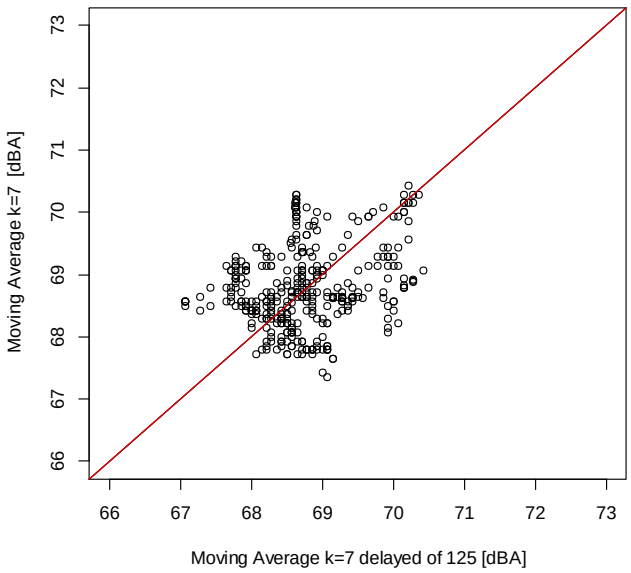

Fig. 4: Auto dispersion plot. The moving average with span 7 is plotted as a function of the same moving average considering each data shifted by 125 days.

B. Double seasonality model design and results

After having established the presence of two seasonal effects, it is possible to remove these periodicities from the data and to evaluate two different seasonal coefficients. Thus, the improved model takes into account the effects of the high frequency seasonality, with a lag of 7 days, but also of the low frequency one, with a lag of 125 days. In Fig. 5, three curves are reported: the actual data (in black), in red the first moving average (span 7), in blue the second moving average (span 125).

In this figure, it is possible to appreciate the combination of the two centred moving averages, that eliminates the double seasonality effects.

The first moving average curve (red curve) highlights the presence of four peaks and valleys. This is an empirical confirmation of the presence of a seasonality of about 500 measurements over 4 peaks/valleys, which is exactly 125.

In Fig. 6, a comparison between the actual data (black line) and the forecasted values of the double seasonality model (DSM) (red line) is presented. Looking at Fig. 6, it is possible to see that the forecasted values fit well the observed one.

C. Models validation

Both the SSM and the DSM have been validated on the 44 days data set, from the 501st to the 544th observations. A graphical comparison has been performed in Fig. 7 and Fig. 8, respectively comparing the SSM and the DSM results with actual data.

A quantitative validation analysis of the models performance has been pursued calculating the difference between actual data and forecasts of the SSM and the DSM. In addition, the distortion and dispersion, measured by the MPE and CVE (see section II), have also been evaluated.

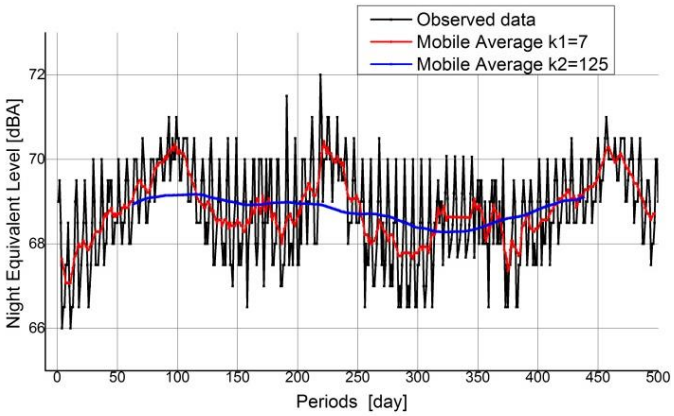

Fig. 5: Graph of the two centred moving averages combination. In black the actual data, in red the first moving average (span 7), in blue the second moving average (span 125).

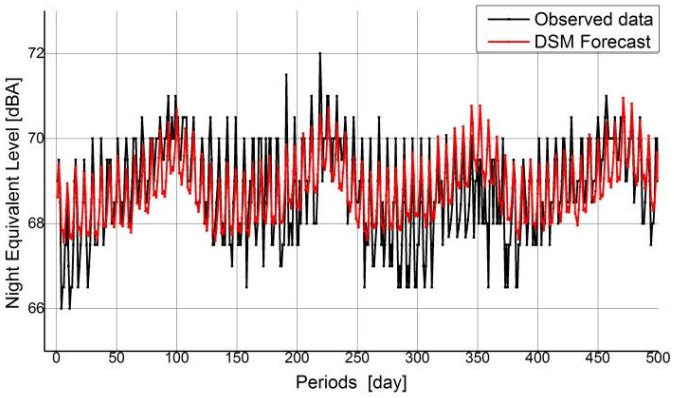

Fig. 6: Comparison between the forecasted values, obtained by DSM, and the 500 calibration data.

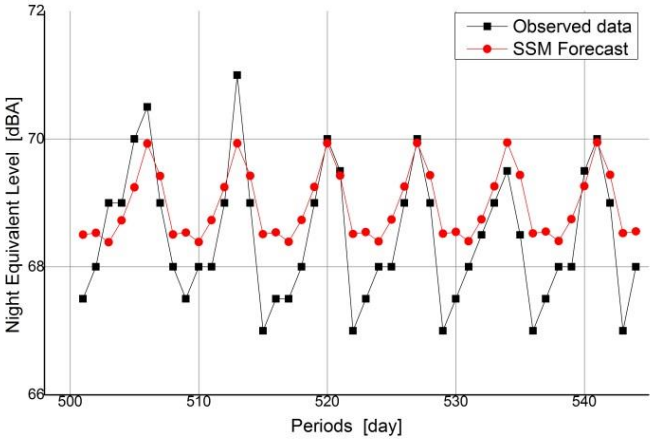

Fig. 7: Comparison between the forecasted values, obtained by SSM model, and the validation with the actual data.

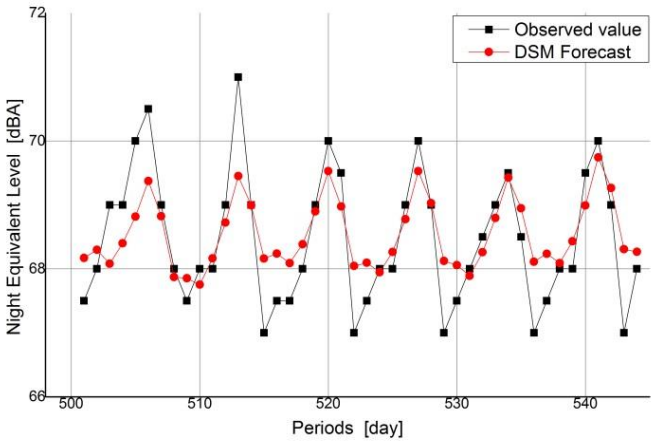

Fig. 8: Comparison between the forecasted values obtained by DSM model, and the validation with the actual data.

The statistics of the error distribution, reported in Tables 3 and 4, show a relevant improvement in the forecasts obtained with the DSM, with respect to SSM results. The absolute values of the mean error strongly decreases, even if the standard deviation is practically the same. In addition, the DSM error distribution approximates well a normal distribution, considering the decreasing (in absolute value) of skewness and kurtosis.

The MPE and CVE results, reported in Table 5, confirm the better performance of DSM. Recall that the calibration error metrics have been evaluated excluding the 26 data obtained by the application of the first model, and considering only the days in which the actual data were available.

Both the graphical and quantitative comparisons between the models show that the DSM has a better performance on the considered set of data, with respect to the SSM.

Table 3: SSM, summary statistics of the error distribution (in dBA) evaluated on the validation.

Mean [dBA]	Std.dev [dBA]	Median [dBA]	Min [dBA]	Max [dBA]	skew	kurt
-0.49	0.62	-0.44	-1.53	1.07	0.29	-0.25

Table 4: DSM, summary statistics of the error distribution (in dBA) evaluated on the validation.

Mean [dBA]	Std.dev [dBA]	Median [dBA]	Min [dBA]	Max [dBA]	skew	kurt
-0.07	0.64	-0.01	-1.31	1.55	0.21	-0.18

Table 5: MPE and CVE (error metrics) values, calculated in the tuning and validation phases, for the two different models.

Type of model	Dataset	MPE	CVE
SSM	tuning	0.0	0.013
SSM	validation	-0.7	0.009
DSM	tuning	0.0	0.011
DSM	validation	-0.1	0.012

D. Error analysis

A statistical analysis of the prediction error, formula (9), is performed on DSM results, by means of the tools presented in section II.D .

The summary statistics of the forecast error of the DSM on the 474 calibration data, i.e. the calibration dataset excluding the 26 missing data, are reported in Table 6, while the error histogram is plotted in Figure 9.

Table 6: Double seasonality model summary statistics of the error distribution evaluated on the calibration dataset.

Mean [dBA]	Std.dev [dBA]	Median [dBA]	Min [dBA]	Max [dBA]	skew	kurt
0.02	0.74	0.15	-3.93	1.99	-0.79	1.72

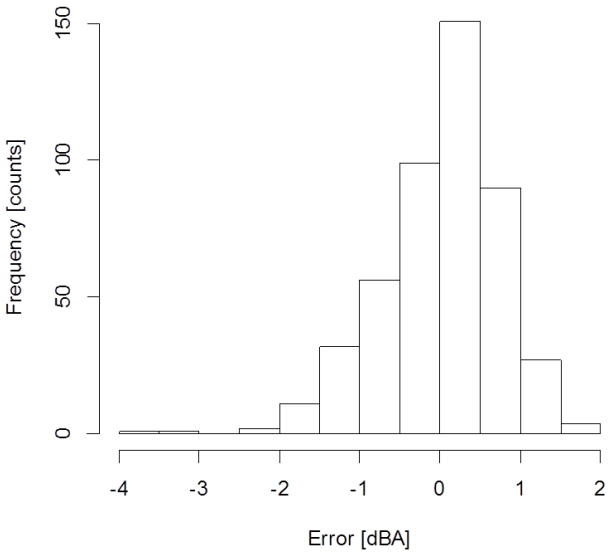

Fig. 9: Frequency histogram of the errors calculated on the model calibration dataset, performed on the 474 dataset.

Using a *t*-test of the "R" software framework, it has been obtained that the average error is not statistically different from zero. In particular, the *t*-statistic calculated on the errors of the DSM, on 474 periods of calibration, is 0.6960518 and the corresponding probability of observing errors in the model, if the null hypothesis of zero mean is true, is 0.2433691. This value is generally considered too high to reject the null hypothesis.

The Shapiro-Wilk and Jarque-Bera tests results are reported in Table 7, while the normality plot of DSM error distribution is presented in Figure 10.

Table 7: Shapiro-Wilk and Jarque-Bera normality tests performed to errors of MDS model applied to the 474 calibration data.

Type of test	Statistic of the test	*df*	p-value
Shapiro-Wilk	0.968	_	1.176 exp(-8)
Jarque-Bera	109.024	2	< 2.2 exp(-16)

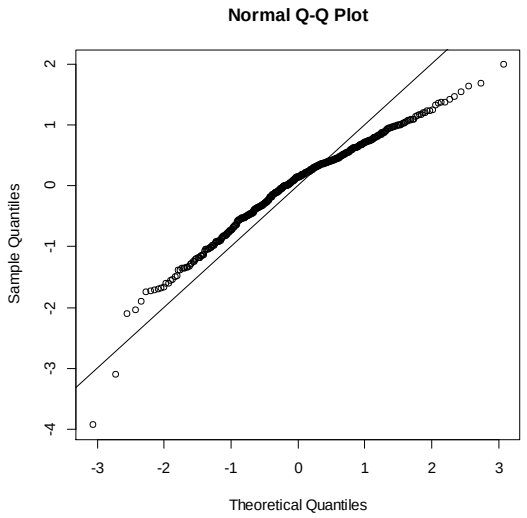

Fig. 10: Normal probability plot that describe error behavior of DS model applied to the 474 calibration data.

The *p*-values reported in Table 7 are very low compared to the levels of significance usually considered in both tests. This makes us lean towards the rejection of the null hypothesis, that is the normality of errors distribution in the calibration phase. This result is in contradiction with the histogram and skewness and kurtosis values. The QQ diagram shows that only a small part of the error distribution quantiles deviates from the bisector line. The SW and JB tests fail, probably due to the sample size.

Performing the *t*-test on the 44 periods of validation, it has been shown that the average error is not statistically different from zero. In particular, the *t*-statistic calculated on the DSM errors is -0.7441655 and the corresponding probability of observing errors in the model the null hypothesis of zero mean is true, is 0.7695881. This value is generally considered too high to reject the null hypothesis. The error histogram and the QQ plot are reported in Fig. 11 and Fig. 12, while the Shapiro-Wilk and Jarque-Bera tests results are reported in Table 8.

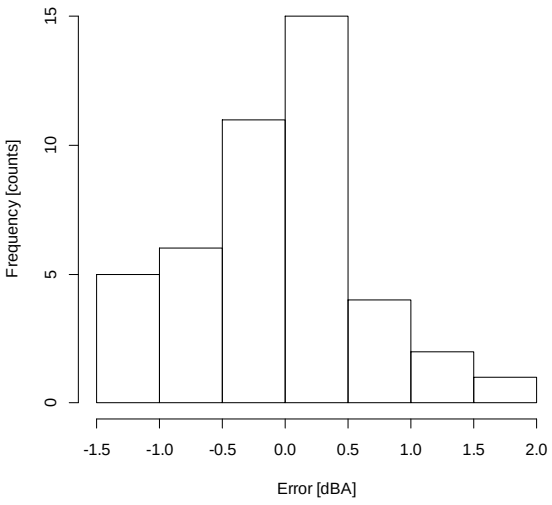

Fig. 11: Frequency histogram of the errors calculated on the model validation, performed on 44 data.

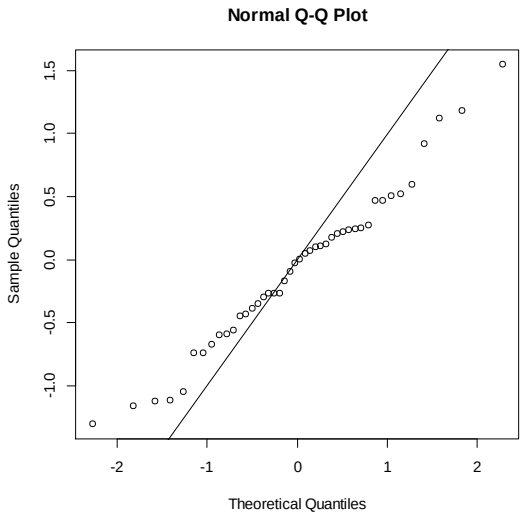

Fig. 12: Normal probability plot that describe error behavior of DSM model applied to the 44 validation data.

Table 8: Shapiro-Wilk and Jarque-Bera Test normality tests performed to errors of MDS model used to predict the 44 validation data.

Type of test	Statistic of the test	*df*	p-value
Shapiro-Wilk	0.9805	-	0.6542
Jarque-Bera	0.3549	2	0.8374

The *p*-values in Tab. 8 are very high compared to the levels of significance which usually are referred to in both statistical tests. That makes us lean towards acceptance of the null hypothesis, that is the normal distribution of errors.

IV. Conclusions

In this work, the attention was focused on the noise pollution monitoring and prediction problem in urban areas. The statistical analysis of a noise levels dataset, obtained from a measuring station in Messina (South Italy), has been performed. These measurements have been adopted for the implementation and validation of a model based on time series analysis. The aim was to predict noise level exposure. This method assumes that the noise level slope is the result of the composition of three parts: a long term behaviour (trend), that is a function of time and is obtained by smoothing the raw data; a seasonal component (seasonality), that describes the periodicities in the phenomenon; and an irregularity, that is not deterministic, but can be probabilistically evaluated. The adopted model is multiplicative between trend and seasonality, and additive when considering the irregularity.

A first set of 321 data has been considered, and, thanks to the application of statistical tests, the presence of periodic variations has been evidenced. Then, a toy model has been implemented on this dataset, considering a weekly periodicity, highlighted by a strong autocorrelation corresponding to a lag value of 7 days.

With the application of this model, a subset of 26 missing measurements has been filled and a 500 dataset has been obtained and analysed. The evaluation of the correlogram on this enlarged dataset confirmed the weekly periodicity (k_1 = 7). Once the trend has been evaluated, by means of centred

moving average (with span equal to 7), the correlogram has been computed on the moving average dataset and a second periodicity has been evidenced. This time, the periodicity is related to a longer term period (k_2 = 125, i.e., about 4 months). Thus, the "single seasonality model" (SSM) has been improved, considering this multiple periodicity evidenced on the entire large dataset, resulting in the "double seasonality model" (DSM). Both SSM and DSM have been validated by comparing their forecasted values with a 44 actual measurement dataset (not used in the calibration phase). These validation data have been also used for a quantitative comparison between the performances of the two models, by means of error (difference between actual value and forecast) distributions. The double seasonality model showed better performances, in terms of lower standard deviation and closer to zero mean value of the error distribution. In addition, the application of normality tests confirmed the hypothesis of normal distribution for the error in the validation dataset.

ACKNOWLEDGMENT

The authors are grateful to the local government of Messina, for making available the long term noise levels measured in the city.

ERR was partially supported by the project PAPIIT-IN102713 of the Direccion General de Apoyo al Personal Academico of the Universidad Nacional Autonoma de Mexico, Mexico.

A shortened version of this work ([45]) was presented at the 2nd Int. Conf. on Acoustics, Speech and Audio Processing (ASAP '14), Salerno, Italy, June 3-5, 2014.

REFERENCES

[1] Kryter KD, *The Effects of Noise on Man*, 2nd edition, Orlando, FL, Academic Press, 1985.

[2] Ouis D., "Annoyance from road traffic noise: a review", *Journal of Environmental Psychology*, Vol. 21, pp. 101-120, 2001.

[3] Guarnaccia C., Mastorakis N. E., Quartieri J., "Noise Sources Analysis in a Wood Manufacturing Company", *International Journal of Mechanics*, Issue 2, Vol. 7, pp 37-44, ISSN: 1998-4448, 2013.

[4] Quartieri J., Troisi A., Guarnaccia C., D'Agostino P., D'Ambrosio S., Iannone G., "Development of an Environmental Quality Index Related to Polluting Agents", *Proceedings of the WSEAS International Conference on "Environment, Ecosystem and Development"* (EED'09), Puerto de la Cruz, Tenerife (Spain), 14-16 December 2009, pp. 153-161.

[5] Rodrigues, E.R., Achcar, J.A., Jara-Ettinger, J., "A Gibbs sampling algorithm to estimate the occurrence of ozone exceedances in Mexico City", in: *Air Quality: Models and Applications*, Popovic D (ed.), in Tech Open Access Publishers, pp. 131-150, (2011).

[6] Achcar, J.A., Fernandez-Bremauntz, A.A., Rodrigues, E.R., Tzintzun, G., "Estimating the number of ozone peaks in Mexico City using a non-homogeneous Poisson model", *Environmetrics*, Vol. 19, pp 469-485, (2008).

[7] Quartieri J., Mastorakis N. E., Iannone G., Guarnaccia C., D'Ambrosio S., Troisi A., Lenza T.L.L, "A Review of Traffic Noise Predictive Models", *Proceedings of the 5th WSEAS International Conference on "Applied and Theoretical Mechanics"* (MECHANICS'09), Puerto de la Cruz, Tenerife, Spain, 14-16 December 2009, pp. 72-80.

[8] Guarnaccia C., Lenza T.LL., Mastorakis N.E., Quartieri J., "A Comparison between Traffic Noise Experimental Data and Predictive Models Results", *International Journal of Mechanics*, Issue 4, Vol. 5, pp. 379-386, ISSN: 1998-4448, (2011).

[9] Guarnaccia C., "Advanced Tools for Traffic Noise Modelling and Prediction", *WSEAS Transactions on Systems*, Issue 2, Vol.12, pp. 121-130, 2013.

[10] Iannone G., Guarnaccia C., Quartieri J., "Speed Distribution Influence in Road Traffic Noise Prediction", *Environmental Engineering And Management Journal*, Vol. 12, Issue 3, pp. 493-501, 2013.

[11] Quartieri J., Iannone G., Guarnaccia C., "On the Improvement of Statistical Traffic Noise Prediction Tools", *Proceedings of the 11th WSEAS International Conference on "Acoustics & Music: Theory & Applications"* (AMTA '10), Iasi, Romania, 13-15 June 2010, pp. 201-207.

[12] Guarnaccia C., "Analysis of Traffic Noise in a Road Intersection Configuration", *WSEAS Transactions on Systems*, Issue 8, Volume 9, pp.865-874, ISSN: 1109-2777, (2010).

[13] Quartieri J., Mastorakis N. E., Guarnaccia C., Troisi A., D'Ambrosio S., Iannone G., "Traffic Noise Impact in Road Intersections", *International Journal of Energy and Environment*, Issue 1, Volume 4, pp. 1-8, (2010).

[14] Iannone G., Guarnaccia C., Quartieri J., "Noise Fundamental Diagram deduced by Traffic Dynamics", in *"Recent Researches in Geography, Geology, Energy, Environment and Biomedicine", Proceedings of the 4th WSEAS Int. Conf. on Engineering Mechanics, Structures, Engineering Geology* (EMESEG '11), Corfù Island, Greece, July 14-16, 2011, pp. 501-507.

[15] Quartieri J., Mastorakis N.E., Guarnaccia C., Iannone G., "Cellular Automata Application to Traffic Noise Control", *Proc. of the 12th Int. Conf. on "Automatic Control, Modelling & Simulation"* (ACMOS '10), Catania (Italy), 29-31 May 2010, pp. 299-304.

[16] Guarnaccia C., "Acoustical Noise Analysis in Road Intersections: a Case Study", *Proceedings of the 11th WSEAS International Conference on "Acoustics & Music: Theory & Applications"* (AMTA '10), Iasi, Romania, 13-15 June 2010, pp. 208-215.

[17] Quartieri J., Troisi A., Guarnaccia C., Lenza TLL, D'Agostino P., D'Ambrosio S., Iannone G., "Analysis of Noise Emissions by Train in Proximity of a Railway Station", *Proceedings of the 10th International Conference on "Acoustics & Music: Theory & Applications"* (AMTA '09), Prague (Rep.Ceca), 23-25 March 2009, pp: 100-107.

[18] Quartieri J., Troisi A., Guarnaccia C., Lenza TLL, D'Agostino P., D'Ambrosio S., Iannone G., "An Italian High Speed Train Noise Analysis in an Open Country Environment", *Proceedings of the 10th International Conference on "Acoustics & Music: Theory & Applications"* (AMTA '09), Prague (Rep.Ceca), 23-25 March 2009, pp: 92-99.

[19] Quartieri J., Troisi A., Guarnaccia C., Lenza TLL, D'Agostino P., D'Ambrosio S., Iannone G., "An Acoustical Study of High Speed Train Transits", *WSEAS Transactions on Systems*, Issue 4, Vol.8, pp. 481-490 (2009).

[20] Quartieri J., Troisi A., Guarnaccia C., Lenza TLL, D'Agostino P., D'Ambrosio S., Iannone G., "Application of a Predictive Acoustical Software for Modelling Low Speed Train Noise in an Urban Environment", *WSEAS Transactions on Systems*, Issue 6, Vol.8, pp. 673-682 (2009).

[21] Quartieri J., Mastorakis N. E., Guarnaccia C., Troisi A., D'Ambrosio S., Iannone G., "Road Intersections Noise Impact on Urban Environment Quality", *Proceedings of the 5th WSEAS International Conference on "Applied and Theoretical Mechanics"* (MECHANICS '09), Puerto de la Cruz, Tenerife, Spain, 14-16 December 2009, pp. 162-171.

[22] Quartieri J., Sirignano L., Guarnaccia C., "Equivalence between Linear and Curved Sources in Newtonian Fields: Acoustics Applications", *Proc. Of the Int. Conf. on Engineering Mechanics, Structures, Engineering Geology* (EMESEG '08), Heraklion, Crete Island, Greece, July 22-24, 2008, pp: 393-395.

[23] Quartieri J., Guida M., Guarnaccia C., D'Ambrosio S., Guadagnuolo D., "Complex Network Applications to the Infrastructure Systems: the Italian Airport Network case", *Proc. of the Int. Conf. on Urban Planning and Transportation* (UPT'07), Heraklion, Crete Island, Greece, July 22-24, 2008, pp: 96-100.

[24] Quartieri J., Mastorakis N.E., Iannone G., Guarnaccia C., "A Cellular Automata Model for Fire Spreading Prediction", in *"Latest Trends on Urban Planning and Transportation", Proc. of the 3rd Int. Conf. on "Urban Planning and Transportation"* (UPT '10), Corfù, Greece, 22-24 July 2010. ISBN: 978-960-474-204-2/ISSN: 1792-4286, pp. 173-179.

[25] Iannone G., Troisi A., Guarnaccia C., D'Agostino P. P., Quartieri J., "An Urban Growth Model Based on a Cellular Automata Phenomenological Framework", *Int. Journal of Modern Physics C*, Volume 22, Issue 05, pp. 543-561. DOI: 10.1142/S0129183111016427, (2011).

[26] Guarnaccia C., Mastorakis N.E., Quartieri J., "Wind Turbine Noise: Theoretical and Experimental Study", *International Journal of Mechanics*, Issue 3, Vol.5, pp. 129-137 (2011).

[27] Quartieri J., Sirignano L., Guarnaccia C., "Infinitesimal Equivalence between Linear and Curved Sources in Newtonian Fields": *Application to Acoustics, International Journal of Mechanics*, Issue 4, Vol.1, pp. 89-91, ISSN: 1998-4448, (2007).
[28] Guarnaccia C., Mastorakis N. E., Quartieri J., "A Mathematical Approach for Wind Turbine Noise Propagation", in *Applications of Mathematics and Computer Engineering, American Conference of Applied Mathematics* (AMERICAN-MATH '11), Puerto Morelos, Mexico, 29-31 January 2011, pp. 187-194.
[29] Brockwell P., Davis R., *Introduction to Time Series and Forecasting* (2nd ed.), Springer, (2002).
[30] Hamilton J.D., *Time Series Analysis*, Princeton University Press, Cloth, 1994.
[31] Box, G. E. P., and Jenkins, G., *Time Series Analysis: Forecasting and Control*, Holden-Day, (1976).
[32] Chatfield, C., *The Analysis of Time Series: An Introduction*, Fourth Edition, Chapman & Hall, New York, NY, (1989).
[33] Directive 2002/49/EC of the European Parliament and of Council of June 25 2002 relating to the assessment and management of environmental noise, Official Journal of the European Communities, L189/12-25,18.7.2002.
[34] Guarnaccia C., Quartieri J., Mastorakis N. E. and Tepedino C., "Acoustic Noise Levels Predictive Model Based on Time Series Analysis", in *"Latest Trends in Circuits, Systems, Signal Processing and Automatic Control", proceedings of the 2nd Int. Conf. on Acoustics, Speech and Audio Processing* (ASAP '14), Salerno, Italy, June 3-5, 2014, ISSN: 1790-5117, ISBN: 978-960-474-374-2, pp. 140-147.
[35] Di Matteo T., Aste T., Dacorogna M.M., "Scaling behaviors in differently developed markets", *Physica A: Statistical Mechanics and its Applications*, Vol. 324, Issues 1–2, pp. 183-188, 2003.
[36] Milanato D., *Demand Planning. Processi, metodologie e modelli matematici per la gestione della domanda commerciale*, Springer, Milano, 2008, in Italian.
[37] Chase R. B., Aquilano N. J., *Operations Management for Competitive Advantage*, Irwin Professional Pub, 10th edition, 2004.
[38] Box, G. E. P., Pierce, D. A., "Distribution of Residual Autocorrelations in Autoregressive-Integrated Moving Average Time Series Models", *Journal of the American Statistical Association*, 65: 1509–1526, (1970).
[39] Ljung G. M., Box, G. E. P., "On a measure of lack of fit in time series models", *Biometrika*, 65, 297-303, (1978).
[40] Chambers, John, William Cleveland, Beat Kleiner and Paul Tukey, *Graphical Methods for Data Analysis*, Wadsworth, 1983.
[41] Shapiro S.S., Wilk M.B., "An Analysis of Variance Test for Normality", *Biometrika* Vol. 52, N. 3/4, pp. 591-611 (1965)
[42] Jarque C. M., Bera A. K., "A test for normality of observations and regression residuals", *International Statistical Review* 55, 163–172 (1987).
[43] Guarnaccia C., Quartieri J., Barrios J. M., Rodrigues E. R., "Modeling environmental noise exceedances using non-homogeneous Poisson processes", *Journal of Acoustical Society of America*, submitted for publication.
[44] http://mobilitamessina.it/index.php/monitoraggio-ambientale
[45] Guarnaccia C., Quartieri J., Rodrigues E. R. and Tepedino C., "Time Series Model Application to Multiple Seasonality Acoustical Noise Levels Data Set", in "*Latest Trends in Circuits, Systems, Signal Processing and Automatic Control", proceedings of the 2nd Int. Conf. on Acoustics, Speech and Audio Processing* (ASAP '14), Salerno, Italy, June 3-5, 2014 , ISSN: 1790-5117, ISBN: 978-960-474-374-2, pp. 171-180.
[46] Guarnaccia C., Quartieri J., Mastorakis N. E., "Comparison of Acoustic Barriers Noise Reductions Evaluated by Different Calculation Methods", *in "Latest Trends on Systems", Proc. of the 18th Int. Conf. on Circuits, Systems, Communications and Computers* (CSCC'14), Santorini, Greece, 17-21 July 2014, pp. 443-449.
[47] Guarnaccia C., Quartieri J., Cerón Bretón J. G., Tepedino C., Cerón Bretón R. M., "Time Series Predictive Model Application to Air Pollution Assessment", *in "Latest Trends on Systems", Proc. of the 18th Int. Conf. on Circuits, Systems, Communications and Computers* (CSCC'14), Santorini, Greece, 17-21 July 2014, pp. 499-505.